HHS Public Access

Author manuscript

Eur J Immunol. Author manuscript; available in PMC 2018 November 01.

Published in final edited form as:

Eur J Immunol. 2017 November ; 47(11): 1925–1935. doi:10.1002/eji.201646904.

Persistent accumulation of gut macrophages with impaired phagocytic function correlates with simian immunodeficiency virus disease progression

Zachary D. Swan[1,3], **Anthea L. Bouwer**[1,3], **Elizabeth R. Wonderlich**[1,3,*], and **Simon M. Barratt-Boyes**[1,2,3]

[1]Department of Infectious Diseases and Microbiology, University of Pittsburgh, Pittsburgh, PA 15261, USA

[2]Department of Immunology, University of Pittsburgh, Pittsburgh, PA 15261, USA

[3]Center for Vaccine Research, University of Pittsburgh, Pittsburgh, PA 15261, USA

Abstract

The contribution of macrophages in the gastrointestinal tract to disease control or progression in HIV infection remains unclear. To address this question, we analyzed CD163+ macrophages in ileum and mesenteric lymph node (LN) from SIV-infected rhesus macaques with dichotomous expression of controlling MHC class I alleles predicted to be SIV controllers or progressors. Infection induced accumulation of macrophages into gut mucosa in the acute phase that persisted in progressors but was resolved in controllers. In contrast, macrophage recruitment to mesenteric LNs occurred only transiently in acute infection irrespective of disease outcome. Persistent gut macrophage accumulation was associated with CD163 expression on α4β7+CD16+ blood monocytes and correlated with epithelial damage. Macrophages isolated from intestine of progressors had reduced phagocytic function relative to controllers and uninfected macaques, and the proportion of phagocytic macrophages negatively correlated with mucosal epithelial breach, lamina propria *E. coli* density and plasma virus burden. Macrophages in intestine produced low levels of cytokines regardless of disease course, while mesenteric LN macrophages from progressors became increasingly responsive as infection advanced. These data indicate that non-inflammatory CD163+ macrophages accumulate in gut mucosa in progressive SIV infection in response to intestinal damage but fail to adequately phagocytose debris, potentially perpetuating their recruitment.

Keywords

Animal models; cellular immunology; HIV; immunopathology; phagocytosis

Corresponding author: Simon M. Barratt-Boyes, 9046 Biomedical Science Tower 3, University of Pittsburgh, 3501 Fifth Avenue, Pittsburgh, Pennsylvania 15261, USA; Phone: 1-412-383-7537; Fax: 1-412-624-4577; smbb@pitt.edu.

*Current address: Southern Research, Frederick, Maryland 21701

Conflict of interest

The authors declare no conflicts of interest.

Introduction

Macrophages are mononuclear phagocytes that mediate innate homeostatic and inflammatory functions in tissues throughout the body. Macrophages are most abundant in the gastrointestinal tract, where they maintain a non-inflammatory environment, expressing low levels of innate response receptors and primarily scavenging debris and promoting wound repair [1, 2]. Under inflammatory conditions, such as with Crohn disease and ulcerative colitis, colonic tissues have an increased frequency of activated proinflammatory macrophages that are hyper-responsive to bacterial stimuli and correlate with increased turnover of CD14-high inflammatory monocytes [3, 4]. These findings have implications for macrophage recruitment and accumulation as a central mechanism in the pathogenesis of inflammatory bowel disorders [5]. Macrophages also infiltrate the intestine in HIV-infected humans and SIV-infected macaques [6–8]. However, whether macrophage accumulation in intestine reflects a beneficial or detrimental role in HIV/SIV pathogenesis remains unknown.

The rhesus macaque MHC class I allele *Mamu-B*008* is correlated with long-term control of SIV replication, generating CD8+ T cell responses against comparable peptides as the human elite controlling allele *HLA-B*27* [9–11]. Macaque controlling alleles *Mamu-A*001* and *Mamu-B*017* are also associated with a low set-point viral load, whereas rhesus macaques that lack expression of all 3 controlling alleles have high set-point virus loads and progress to disease in a predictable fashion [12–14]. Hence, by using SIV-infected rhesus macaques with or without expression of protective MHC class I alleles, immune responses in animals predicted to control or progress to disease based on viral set-point can be examined in the same species of monkey infected with the same strain of virus. In this study, we used differential expression of SIV controlling alleles to explore the potential contribution of gut macrophages during acute and chronic stages of infection to disease progression or control.

Our findings reveal that CD163+ macrophages accumulate in ileal mucosa but not mesenteric lymph node (LN) at all stages of progressive SIV infection in association with intestinal damage. These gut macrophages have reduced phagocytic capacity and fail to clear debris, providing a positive feedback for sustained macrophage recruitment. The findings also reveal that gut macrophages in both SIV progressors and controllers, in contrast to macrophages in mesenteric LNs, do not spontaneously release proinflammatory cytokines in chronic infection and do not respond to viral stimuli *ex vivo*. These findings suggest that CD163+ gut macrophages may serve to limit the inflammatory response in progressive infection rather than promote it.

Results

Persistent accumulation of macrophages in small intestine in macaques with progressive SIV infection

We developed a model of diverging SIV disease course in rhesus macaques using differential expression of protective MHC molecule *Mamu-B*008* [9]. We identified 12 rhesus macaques with and 12 without expression of *Mamu-B*008* based on a pre-study haplotype screen. Of the 12 that expressed *Mamu-B*008*, 3 co-expressed controller allele *Mamu-*

*A*001* and 1 animal expressed alleles *Mamu-B*008, A*001, and B*017*. *Mamu-B*008*-negative macaques also lacked expression for *Mamu-A*001* and *Mamu-B*017* (Table 1). Macaques were inoculated intrarectally with a single high dose (10^5 $TCID_{50}$) of pathogenic isolate SIVmac251 and monitored out to week 20 post-infection. A threshold of 10^4 SIV RNA copies/mL plasma at virus load set-point (week 8) was used to sort animals into predicted SIV progressors or controllers [15]. In total, 14 macaques had set-point virus loads $>10^4$ SIV RNA copies/mL and were defined as SIV progressors and 10 had set-point virus loads $<10^4$ SIV RNA copies/mL and were defined as SIV controllers (Table 1). Viral load divergence in the two groups was statistically significant by week 3 post-infection (Fig. 1A).

We first evaluated the frequency of macrophages in the ileum using established *in situ* techniques [8]. In parallel, we identified and analyzed macrophage frequency in mesenteric LNs by flow cytometry, gating on CD3/CD20–MHC class II+CD163+ cells [8]. We used scavenger receptor CD163 to define macrophages based on its restriction to cells of monocyte/macrophage lineage including macrophages in the intestine [1] and the extensive literature regarding CD163+ cells and soluble CD163 in HIV/SIV pathogenesis [6, 8, 16–22]. The density of CD163+ macrophages increased over 2-fold in both the mesenteric LNs and gut mucosa in acute SIV infection compared with pre-infection (Fig. 1B, C). By week 12, the proportion of macrophages in mesenteric LNs had declined to pre-infection levels. However, in gut there was a stark divergence in macrophage abundance between controllers, which had a decline in the frequency of macrophages, and progressors, which had a persistently high frequency of macrophages. This difference achieved statistical significance at week 20 (Fig. 1C, D). Gut macrophage frequency at weeks 12 and 20 strongly correlated with the level of chronic phase plasma viremia (Fig. 1C).

We next generated single-cell suspensions of ileum and used flow cytometry to explore changes in gut macrophage activation and turnover between progressors and controllers. Gut macrophages were identified as CD3/CD20–MHC class II+CD163+ cells and assessed for expression of Ki67, a measure of recent cell division, activation markers CD86 and CD95, and active caspase-3 and caspase-1, regulators of cell death pathways apoptosis and pyroptosis, respectively (Fig. 1E). Infection with SIV had no influence on the frequency of gut macrophages expressing Ki67, CD86, or active caspase-3, however there was a trend towards increased active caspase-1 expression in the chronic stage in both progressors and controllers. The proportion of CD95+ macrophages increased during acute infection in both groups and remained somewhat elevated in progressors at chronic stages (Fig. 1F).

To determine if monocyte trafficking represented a potential mechanism for increased macrophages in SIV-infected intestine, we stained PBMC for CD14 and CD16 to delineate the three monocyte subsets found in blood and assessed for expression of gut-homing integrin α4β7 by flow cytometry (Supplemental Fig. 1A). Monocytes were identified as CD16–CD14+, CD16+CD14+, or CD16+CD14− within the MHC class II+ population lacking expression for CD3, CD20, and CD8 [23]. Prior to infection, all monocyte subsets expressed low levels of α4β7. After infection both SIV controllers and progressors had an increased frequency of α4β7+CD16+CD14− monocytes at week 2 post-inoculation that declined by chronic infection and was not significant between groups (Supplemental Fig. 1A, B). The proportion of α4β7+CD16–CD14+ monocytes also increased in progressors

during the acute stage. To evaluate if gut-homing monocytes could be a source of accumulating CD163+ macrophages, we next looked at expression of CD163 on α4β7+ monocytes. Consistent with previous reports, the CD16+CD14− subset expressed the lowest level of CD163 in uninfected blood, whereas expression of CD163 on CD16+CD14+ and CD16–CD14+ monocytes was nearly 5-fold higher by comparison [24]. Notably, CD163 expression was selectively elevated on all α4β7+ monocytes in macaques with progressive SIV infection during the acute phase compared to controllers and remained elevated at week 12 only on the CD16+CD14− subset (Supplemental Fig. 1C).

Progressive SIV infection is associated with increased intestinal breach and microbial translocation

We next sought to investigate the relationship between macrophage frequency in the gut and intestinal epithelial barrier damage and microbial translocation [25]. Sections of ileum were stained with Ab to cytokeratin to assess intestinal epithelial integrity and Ab to *Escherichia coli* (*E.coli*) to assess microbial translocation [25]. Tissues taken prior to infection displayed uniform staining for cytokeratin along the interface of the lumen and lamina propria reflecting an uncompromised barrier of columnar epithelial cells. At week 2 of infection, multifocal disruptions in cytokeratin expression were present in both cohorts of animals (Fig. 2A). Qualitative and quantitative analysis revealed a pronounced disruption of cytokeratin expression by weeks 12 and 20 in SIV progressors that was not apparent in macaques with controlled infection (Fig. 2A, B). Shortened intestinal villi were also evident in sections of gut from progressor animals at the chronic stages, consistent with villous atrophy noted in HIV enteropathy [26]. Evidence of microbial translocation as measured by *E.coli* staining was sparse in the intestinal lamina propria prior to infection, with the majority of *E.coli* present on the luminal side of the gut (Fig. 2A). Infection was associated with an increase in the percentage of lamina propria occupied by *E.coli*, primarily among SIV progressors, however there was considerable variation between animals (Fig. 2B). Increased intestinal damage in chronic infection strongly correlated with macrophage abundance and chronic phase viremia, but not microbial translocation (Fig. 2C).

Gut macrophages in progressive SIV infection have impaired phagocytic function

Next we used confocal microscopy to analyze *in situ* whether accumulating macrophages phagocytose cellular and bacterial debris in small intestine. Sections of ileum were stained with Abs to CD163 and either cytokeratin, *E.coli*, or hemoglobin, the biological ligand for CD163, and then analyzed for co-expression, a measure of macrophage phagocytosis. Staining for cytokeratin in infected gut, particularly in regions with intestinal breach, revealed cytokeratin+ debris within the lamina propria where large clusters of macrophages could also be found. Co-staining for CD163 and lamina propria-associated cytokeratin could be detected in SIV-infected tissues but was seldom seen before infection (Fig. 3A, top). In contrast, co-localization of CD163 with *E.coli*+ staining was rare in both uninfected and infected intestine, even in tissues where microbial translocation was most abundant (Fig. 3A, middle). Hemoglobin staining was plentiful in infected gut, suggestive of focal hemorrhage and hemolysis, and confocal imaging revealed hemoglobin deposits within CD163+ macrophages (Fig. 3A, bottom).

To quantitatively address the impact of SIV infection on macrophage phagocytic function, we next assessed the ability of isolated gut macrophages to engulf antigen *ex vivo*. Phagocytosis was determined by measuring real-time uptake of fluorescently-labeled bioparticles using a pH-sensitive assay. Intestinal suspensions from before infection and at week 20 post-infection were incubated with bioparticles and then stained with Abs for detection of phagocytic macrophages by flow cytometry. Macrophages expressing CD163 were delineated in suspension and phagocytic macrophages identified as pHrodo+ (Fig. 3B). We also analyzed bioparticle uptake in macrophages from mesenteric LNs for comparison. Phagocytic macrophages in gut represented a median 27% of the total CD163+ population prior to infection, and roughly twice as many macrophages could uptake antigen in mesenteric LNs (Fig. 3C). After infection, however, we found a dramatic decline in bioparticle uptake by intestinal macrophages at week 20 in SIV progressors compared to macrophages in SIV controllers and uninfected macaques. In contrast, we found no change in mesenteric LN macrophage's ability to phagocytose bioparticles with infection (Fig. 3C). The frequency of phagocytic macrophages in gut mucosa inversely correlated with gut macrophage abundance, intestinal breach, lamina propria *E.coli* density and chronic phase viral load (Fig. 3D).

We next quantified cell-associated virus in mesenteric LNs and intestine by RT-PCR as well as determined the percentage of SIV p27 (gag)+ macrophages in suspension by flow cytometry. In both mesenteric LNs and gut, there was a trend towards more cell-associated virus in progressors compared to controllers at week 20 (Fig. 3E). Nevertheless, flow cytometric analysis of p27+ cells revealed infected macrophages were rare in both mesenteric LN and ileum at week 20 post-infection regardless of disease outcome (Fig. 3F).

Gut macrophages are poor producers of inflammatory cytokines regardless of SIV infection

We next evaluated whether increased macrophages in SIV-infected gut mucosa may contribute to gut-associated inflammation. To address this question, we assessed the capacity of CD163+ macrophages in suspension to respond to *ex vivo* stimulation with aldrithiol-2-inactivated SIV (iSIV) that activates macrophages through TLR8, and influenza virus, which can stimulate RIG-I and TLR3, 7, and 8 [27–29]. We also stimulated macrophages with Env976, a uridine rich ssRNA oligonucleotide sequence derived from SIVmac251 *env* gene that stimulates macrophages through TLR8 (Fig. 4A) [30]. In uninfected mesenteric LNs, macrophages were moderately responsive to Env976 and iSIV stimulations but not influenza and produced low levels of cytokines spontaneously (Fig. 4B). Following infection, there was a non-significant increase in the frequency of macrophages spontaneously producing cytokines that was sustained into chronic infection. Similar changes in cytokine+ macrophages were seen after *ex vivo* stimulation during the acute stage, however the proportions were comparable to the level of cytokines produced spontaneously. By week 20 post-infection, macrophages from progressors were significantly more responsive to Env976 and iSIV compared to controllers (Fig. 4B). In comparison, in gut mucosa, the percentage of unstimulated or stimulated gut macrophages producing combinations of TNF-α, IFN-α, and/or IL-6 was below 5% in macaques before to infection (Fig. 4C). SIV progressors exposed to Env976 had significantly more cytokine+ macrophages at week 12 compared to

pre-infection and week 2; a finding not observed in macrophages from animals with low set-point viral loads. Nevertheless, differences in gut were minor, especially compared to in mesenteric LNs, and overall very few intestinal macrophages produced any combination of TNF-α, IFN-α, or IL-6 spontaneously or in response to iSIV or influenza after infection regardless of predicted disease outcome (Fig. 4C).

Discussion

In this study, we report differences in macrophage abundance and function in ileum of SIV-infected rhesus macaques with differential disease outcome that exist during chronic infection and correlate with the degree of gut epithelial damage. In contrast to macrophages that dominate colon in inflammatory bowel disease, we found no evidence of a proinflammatory response from infiltrating macrophages in SIV-infected animals with progressive disease [3, 31–33]. Instead, macrophages in the ileum of SIV-infected macaques were non-responsive to viral agonists and had decreased phagocytic capacity in progressors but not controllers. These longitudinal data expand upon cross-sectional findings in HIV-infected humans and SIV-infected macaques [6–8] and suggest that increased intestinal pathology in progressive disease is a mechanism of recruitment for macrophages into gut. The data further suggest that failure of gut macrophages to phagocytose debris promotes their continued recruitment and infiltration.

The cause of intestinal macrophage dysfunction in animals with progressive SIV infection is unclear but is likely to be multifactorial. Macrophages are secondary reservoirs of HIV/SIV in the gastrointestinal tract and support infection and active replication of virus in explanted vaginal mucosa [34]. In small intestine, however, macrophages lack surface receptors CD4, CCR5, and CXCR4 for viral entry and are not permissive to infection [35], consistent with our data. Animals with controlled SIV infection in our study had minimal intestinal damage and microbial translocation, comparable to findings in nonpathogenic SIV models that have less systemic immune activation and tissue-associated inflammation despite high levels of virus replication in blood and gut [36, 37]. Together, these results suggest that altered macrophage phagocytic activity in SIV-infected small intestine is likely a consequence of the state of the local microenvironment and not direct viral infection.

We used CD163 to identify macrophages in the ileum as the majority of macrophages in the human gut express this receptor [1]. Other studies in HIV infection have used CD68 in parallel with CD163 to identify macrophages in the duodenal mucosa and found nearly identical proportions of macrophages when either marker was used [6]. The pan-myeloid marker CD33 can be used to identify intestinal macrophages in the human but this marker is also found on dendritic cell subsets [38]. Functionally, CD163 senses bacterial antigen and excessive hemoglobin deposits from lysed blood cells and promotes their uptake and degradation [39]. Our findings of increased non-inflammatory macrophages in animals with intestinal breach suggest a role for macrophage recruitment and phagocytosis in mitigating tissue-associated inflammation and subsequent intestinal barrier breakdown [40]. Microbial translocation is a hallmark of HIV/SIV infection and a cause of chronic immune activation associated with progression to AIDS, and studies in HIV-infected humanized mice demonstrate a link between impaired macrophage phagocytic function, plasma LPS burden,

and systemic T cell activation [41, 42]. Less appreciated are the effects of macrophage functional impairment on clearing excessive hemoglobin in tissues, which could have equally important pathologic consequences due to hemoglobin's ability to induce leukocyte production of TNF-α, IL-8, and IL-6 that may further trigger enterocyte apoptosis [43].

In health, intestinal macrophages downregulate TLR-adaptor proteins MyD88 and TRIF as well as other innate signaling molecules in response to stromal-derived TGF-β and IL-10 to avoid adverse reactions towards enteric microbiota [2]. Previous studies have shown that TGF-β and IL-10 expression levels are elevated in HIV/SIV-infected gut mucosa, and therefore these cytokines could potentially continue to act on newly recruited macrophages to promote a non-inflammatory phenotype [44]. In our study, macrophages in mesenteric LNs but not gut mucosa from SIV progressors became increasingly responsive to stimulation by virus-encoded ligands, suggesting an enhanced ability to respond to pathogens as infection advances. It is not clear whether other subsets of macrophages might accumulate in SIV-infected mucosal tissues and contribute to inflammation. In HIV infection, CD14+ macrophage numbers are increased in colon from AIDS patients and express TNF-α and IL-1β, but whether these cells also express CD163 was not addressed [45]. It is also possible that gut macrophages in animals with a progressive disease course switch to have an inflammatory function with the onset of AIDS [8].

Our results suggest that macrophage accumulation in intestine derives from extravasated monocytes co-expressing CD163 and gut-homing marker α4β7. Plasmacytoid dendritic cells in blood similarly upregulate α4β7 during SIV infection and accumulate in rectal tissues [46]. Others have reported that the frequency of CD163+CD16+ monocytes correlates positively with viral burden in HIV infection, and that *in vitro* maturation of monocytes into macrophages induces CD163 expression [24, 47]. Macrophage activation is associated with increased shedding of membrane-bound CD163, and increased soluble CD163 in plasma is characteristic of AIDS pathogenesis [20, 22]. LPS-induced shedding of CD163 from monocytes indicates CD14+ monocytes may contribute a majority of CD163 in plasma [24]. Previous studies reveal that CD16+CD14− monocytes are preferentially expanded in acute and chronic SIV infection and share functional characteristics with intestinal CD163+ macrophages in our study [48, 49]. In Crohn disease patients, classical CD14+ monocytes selectively migrate to inflamed colon and phenotypically and functionally resemble newly accumulated CD14+ inflammatory macrophages [4]. CD14+CD16+ macrophages expressing high levels of M-DC8, a variant of P-selectin glycoprotein ligand-1, are abundant in inflamed tissues of Crohn patients [50]. Notably, circulating activated M-DC8+ monocytes that over-produce TNF-α in response to microbial products are seen in untreated and viremic HIV-infected individuals [51]. Whether these activated M-DC8+ monocytes that reportedly lack CD163 expression accumulate in gut mucosa is currently not known. It is notable that blockade of α4β7 in combination with antiretroviral therapy promotes virologic control better than antiretroviral drugs alone [52]. Given our findings, it is likely this therapeutic approach might also impact macrophage recruitment to gut mucosal tissues.

Gut macrophages had not undergone high levels of recent cell division in response to SIV infection in our study. Macrophages in acute SIV-infected LNs also undergo limited proliferation but significant cell division is found in LNs taken much later in infection (≥66

weeks post-SIV) and in AIDS [8, 53, 54]. Our data show a trend towards increased macrophage expression of caspase-1 as infection progresses, suggesting that pyroptosis, which is a downstream effect of caspase-1 activation, may be a feature in gut macrophage death as it is in CD4+ T cells in HIV-infected LNs [55]. The potential contributions of pyroptosis and apoptosis to macrophage death in gut mucosa need to be further addressed.

In summary, we have used dichotomous expression of controlling MHC class I alleles to show that macrophages with reduced phagocytic function persistently accumulate in the small intestinal mucosa in progressive SIV infection associated with tissue damage. Presumably, the capacity of virus-specific CD8+ T cells to reduce virus load and virus-mediated tissue destruction in controllers allowed for normal macrophage recruitment and function in gut mucosa in this group. Whether antiretroviral therapy would have the same effect on macrophage function is not known; however antiretroviral therapy does prevent the massive accumulation of gut macrophages that otherwise occurs in untreated HIV patients [6].

Materials and methods

Animal procedures

Indian-origin rhesus macaques housed at the University of Pittsburgh (U.S. Public Health Service Assurance Number: A3187-01) were used in this study and all animal manipulations and procedures were done with appropriate institutional regulatory oversight and approval. Twelve macaques were selected with and 12 without expression of *Mamu-B*008*, a macaque MHC class I allele correlated with control of chronic phase plasma viral burden [9]. Macaques were inoculated intrarectally with 10^5 $TCID_{50}$/mL of SIVmac251 and plasma was extracted from whole blood drawn periodically to monitor viral burden and for analysis of cells in circulation. Mesenteric LNs and resections of ileum of approximately 20–25cm in length were taken from each animal using well-established techniques [56] at two of the following time-points: pre-infection, or at weeks 2, 12, or 20 post-inoculation. Briefly, animals were anesthetized with isoflurane and a ventral midline incision was made to exteriorize the small intestine and associated mesentery. A section of ileum was isolated using intestinal clamps and resected and the two ends anastomosed surgically. Individual mesenteric LNs were excised from the mesentery and the rent in the mesentery was sutured closed. No adverse effects were noted following these resections beyond initial inappetance and discomfort which was alleviated palliatively with analgesics. A minimum of 8 weeks was allowed between repeat surgeries.

Tissue preparation

For isolation of mononuclear cells from intestine, tissues were minced and incubated in 5mM EDTA HBSS. Intestinal slurries were subsequently digested in 15 U/mL collagenase media, mechanically disrupted, and run on a Percoll gradient for leukocyte separation. Suspensions of freshly isolated mesenteric LNs were generated as previously described [8]. Viral RNA in mesenteric LNs and intestinal suspensions was determined using RT-PCR and quantified per 1×10^6 cells. A portion of resected intestine was fixed in 2% paraformaldehyde and infused with 30% sucrose prior to freezing with an aerosol of chlorodifluoromethane

and stored at −80°C. Viral RNA in plasma was determined by RT-PCR as previously described [57].

Immunofluorescence microscopy and quantitative analysis

Sections of ileum were prepared and stained as described previously [8] using the following primary Ab: monoclonal mouse anti-human Cytokeratin (Clone MNF116, Dako), rabbit polyclonal anti-*E.coli* (Dako), monoclonal rabbit anti-hemoglobin (EPR3608, abcam), and monoclonal mouse anti-human CD163 Biotin (GHI/61, eBioscience). Primary Ab were detected using secondary Ab from Thermo Scientific: donkey-anti-rabbit IgG Alexa Fluor 546 secondary, goat anti-mouse Alexa Fluor 546, and HRP-Streptavidin Alexa Fluor 488 Tyramide Signal Amplification kits. *In situ* quantification for CD163+ macrophages, cytokeratin, and *E.coli* was carried out as previously published by us and others [8, 25]. To determine intestinal breach, the length of the epithelial interface between the lumen and lamina propria with and without cytokeratin expression was assessed using the length measurement tool in NIS-Elements software (Nikon). Percent breach was then ascertained using the formula: ((length of no cytokeratin expression) / (length of no cytokeratin expression + length of cytokeratin expression)) × 100. Percent area of *E.coli* was determined by tracing using the NIS-Elements polygonal ROI function. Percent *E.coli*+ area was calculated using the formula: (area of lamina propria occupied by *E.coli* staining / total area of lamina propria) × 100. All data represent averages of quantification from ten nonoverlapping regions of lamina propria.

Flow cytometry and phagocytosis assay

Ileum, mesenteric LNs, and PBMC suspensions were stained with the following cell surface-labeling anti-human Ab (all Ab were purchased from BD Biosciences unless otherwise noted): HLA-DR (clone L243), CD163 (GHI/61), CD3 (SP34-2), CD4 (L200), CD20 (2H7, eBioscience), CD45 (D058-1283), CD14 (M5E2), CD16 (3G8), CD8 (RPA-T8), p27 (55-2F12, NIH AIDS Reagents), CD86 (FUN-1), CD95 (DX2), and α4β7 (A4B7, NHP Reagent Resource). Nonviable cells were excluded with a fluorescent LIVE/DEAD cell stain (Invitrogen). Intracellular analysis of Ki67 (B56) and active caspase-3 (C92-605) were conducted after permeabilization with Cytofix/Cytoperm reagent (BD Biosciences). Detection of active caspase-1 was carried out using the FAM-FLICA Caspase-1 Assay Kit (ImmunoChemistry Technologies) per the manufacturer's instructions. To measure responses to stimulation, freshly isolated intestinal and mesenteric LN single cell suspensions were cultured for 7 h with H7N3 influenza virus (MOI of 5), Env976 oligonucleotides (10μg/mL), or AT-2 iSIVmac239 (200ng capsid/mL) with or without brefeldin A (Sigma) treatment after 2 h before cell surface labeling. Cells were then fixed and permeabilized using Cytofix/Cytoperm and subsequently stained with anti-human Ab to TNF-α (Mab11), IL-6 (MQ2-6A3), and IFN-α (225.C, Chromaprobe). Phagocytic activity was determined using the pHrodo *Escherichia coli* BioParticles Conjugate for Phagocytosis kit (Invitrogen) according to the manufacturer's instructions with minor modifications. Briefly, a suspension of 2×10^6 intestinal cells were incubated at 4°C or 37°C for 1 h in a fixed volume of media before the addition of 50μL pHrodo for an additional 1 h. Cells were subsequently washed and stained with surface markers for macrophage identification. All

data were acquired using an LSR II flow cytometer (BD Biosciences) and analyzed using FlowJo 7.6.4 (TreeStar).

Statistical analysis

Cross-sectional comparisons between SIV progressors and controllers were performed using a regular two-way ANOVA followed by Sidak's post test. Longitudinal comparisons across multiple timepoints were performed using a nonparametric one-way ANOVA followed by Dunn's post test. Comparisons between two timepoints (e.g., pre-infection vs. week 20) were performed using a two-tailed nonparametric Mann-Whitney U test. Correlations were determined using a two-tailed nonparametric Spearman rank test. All aforementioned statistical tests were carried out using GraphPad Prism version 6. Pie charts were analyzed using a permutation test performed with SPICE (version 5.22). A p-value < 0.05 was considered significant.

Supplementary Material

Refer to Web version on PubMed Central for supplementary material.

Acknowledgments

The authors thank Anita M. Trichel for performing gut surgeries, Amanda P. Smith, Timothy J. Sturgeon and Ivona Pandrea for technical assistance, Simon C. Watkins and the Center for Biologic Imaging of the University of Pittsburgh for confocal microscopy and image analysis, and R. Keith Reeves for providing his protocol for processing gut tissue. We also thank Jeffrey D. Lifson of AIDS and Cancer Virus Program, SAIC-Frederick for supplying inactivated SIV, Ronald L. Brown of Quality Biological, Inc. and Jonathan Warren of the Vaccine Research Program, NIAID Division of AIDS for their contribution of SIVmac251 inoculum. This work was funded by US National Institutes of Health grant R01 AI071777 to SMBB and 1S10OD019973-01 to the Center for Biologic Imaging. ZDS was supported by US National Institutes of Health training grant T32 AI065380 and ERW was supported by National Cancer Institute training grant T32 CA082084.

Abbreviations

LN lymph node

References

1. Bain CC, Mowat AM. Macrophages in intestinal homeostasis and inflammation. Immunol Rev. 2014; 260:102–117. [PubMed: 24942685]
2. Smith PD, Smythies LE, Shen R, Greenwell-Wild T, Gliozzi M, Wahl SM. Intestinal macrophages and response to microbial encroachment. Mucosal immunology. 2011; 4:31–42. [PubMed: 20962772]
3. Kamada N, Hisamatsu T, Okamoto S, Chinen H, Kobayashi T, Sato T, Sakuraba A, et al. Unique CD14 intestinal macrophages contribute to the pathogenesis of Crohn disease via IL-23/IFN-gamma axis. J Clin Invest. 2008; 118:2269–2280. [PubMed: 18497880]
4. Thiesen S, Janciauskiene S, Uronen-Hansson H, Agace W, Hogerkorp CM, Spee P, Hakansson K, et al. CD14(hi)HLA-DR(dim) macrophages, with a resemblance to classical blood monocytes, dominate inflamed mucosa in Crohn's disease. J Leukoc Biol. 2014; 95:531–541. [PubMed: 24212097]
5. Heinsbroek SE, Gordon S. The role of macrophages in inflammatory bowel diseases. Expert Rev Mol Med. 2009; 11:e14. [PubMed: 19439108]

6. Allers K, Fehr M, Conrad K, Epple HJ, Schurmann D, Geelhaar-Karsch A, Schinnerling K, et al. Macrophages accumulate in the gut mucosa of untreated HIV-infected patients. The Journal of infectious diseases. 2014; 209:739–748. [PubMed: 24133185]
7. Ortiz AM, DiNapoli SR, Brenchley JM. Macrophages are phenotypically and functionally diverse across tissues in simian immunodeficiency virus-infected and uninfected asian macaques. J Virol. 2015; 89:5883–5894. [PubMed: 25787286]
8. Swan ZD, Wonderlich ER, Barratt-Boyes SM. Macrophage accumulation in gut mucosa differentiates AIDS from chronic SIV infection in rhesus macaques. Eur J Immunol. 2016; 46:446–454. [PubMed: 26549608]
9. Loffredo JT, Maxwell J, Qi Y, Glidden CE, Borchardt GJ, Soma T, Bean AT, et al. Mamu-B*08-positive macaques control simian immunodeficiency virus replication. J Virol. 2007; 81:8827–8832. [PubMed: 17537848]
10. Mudd PA, Ericsen AJ, Burwitz BJ, Wilson NA, O'Connor DH, Hughes AL, Watkins DI. Escape from CD8(+) T cell responses in Mamu-B*00801(+) macaques differentiates progressors from elite controllers. J Immunol. 2012; 188:3364–3370. [PubMed: 22387557]
11. Loffredo JT, Sidney J, Bean AT, Beal DR, Bardet W, Wahl A, Hawkins OE, et al. Two MHC class I molecules associated with elite control of immunodeficiency virus replication, Mamu-B*08 and HLA-B*2705, bind peptides with sequence similarity. J Immunol. 2009; 182:7763–7775. [PubMed: 19494300]
12. Muhl T, Krawczak M, Ten Haaft P, Hunsmann G, Sauermann U. MHC class I alleles influence set-point viral load and survival time in simian immunodeficiency virus-infected rhesus monkeys. J Immunol. 2002; 169:3438–3446. [PubMed: 12218167]
13. Lim SY, Chan T, Gelman RS, Whitney JB, O'Brien KL, Barouch DH, Goldstein DB, et al. Contributions of Mamu-A*01 status and TRIM5 allele expression, but not CCL3L copy number variation, to the control of SIVmac251 replication in Indian-origin rhesus monkeys. PLoS Genet. 2010; 6:e1000997. [PubMed: 20585621]
14. Smith SM, Holland B, Russo C, Dailey PJ, Marx PA, Connor RI. Retrospective analysis of viral load and SIV antibody responses in rhesus macaques infected with pathogenic SIV: predictive value for disease progression. AIDS Res Hum Retroviruses. 1999; 15:1691–1701. [PubMed: 10606092]
15. Mudd PA, Ericsen AJ, Burwitz BJ, Wilson NA, O'Connor DH, Hughes AL, Watkins DI. Escape from CD8(+) T cell responses in Mamu-B*00801(+) macaques differentiates progressors from elite controllers. Journal of immunology. 2012; 188:3364–3370.
16. Borda JT, Alvarez X, Mohan M, Hasegawa A, Bernardino A, Jean S, Aye P, et al. CD163, a marker of perivascular macrophages, is up-regulated by microglia in simian immunodeficiency virus encephalitis after haptoglobin-hemoglobin complex stimulation and is suggestive of breakdown of the blood-brain barrier. Am J Pathol. 2008; 172:725–737. [PubMed: 18276779]
17. Filipowicz AR, McGary CM, Holder GE, Lindgren AA, Johnson EM, Sugimoto C, Kuroda MJ, et al. Proliferation of perivascular macrophages contributes to the development of encephalitic lesions in HIV-infected humans and in SIV-infected macaques. Sci Rep. 2016; 6:32900. [PubMed: 27610547]
18. Fischer-Smith T, Tedaldi EM, Rappaport J. CD163/CD16 coexpression by circulating monocytes/macrophages in HIV: potential biomarkers for HIV infection and AIDS progression. AIDS research and human retroviruses. 2008; 24:417–421. [PubMed: 18373432]
19. Walker JA, Sulciner ML, Nowicki KD, Miller AD, Burdo TH, Williams KC. Elevated numbers of CD163+ macrophages in hearts of simian immunodeficiency virus-infected monkeys correlate with cardiac pathology and fibrosis. AIDS Res Hum Retroviruses. 2014; 30:685–694. [PubMed: 24524407]
20. Knudsen TB, Ertner G, Petersen J, Moller HJ, Moestrup SK, Eugen-Olsen J, Kronborg G, et al. Plasma soluble CD163 level independently predicts all-cause mortality in HIV-1-infected individuals. J Infect Dis. 2016; 214:1198–1204. [PubMed: 27354366]
21. Burdo TH, Soulas C, Orzechowski K, Button J, Krishnan A, Sugimoto C, Alvarez X, et al. Increased monocyte turnover from bone marrow correlates with severity of SIV encephalitis and CD163 levels in plasma. PLoS pathogens. 2010; 6:e1000842. [PubMed: 20419144]

22. Burdo TH, Lentz MR, Autissier P, Krishnan A, Halpern E, Letendre S, Rosenberg ES, et al. Soluble CD163 made by monocyte/macrophages is a novel marker of HIV activity in early and chronic infection prior to and after anti-retroviral therapy. J Infect Dis. 2011; 204:154–163. [PubMed: 21628670]
23. Sugimoto C, Hasegawa A, Saito Y, Fukuyo Y, Chiu KB, Cai Y, Breed MW, et al. Differentiation kinetics of blood monocytes and dendritic cells in macaques: insights to understanding human myeloid cell development. J Immunol. 2015; 195:1774–1781. [PubMed: 26179903]
24. Tippett E, Cheng WJ, Westhorpe C, Cameron PU, Brew BJ, Lewin SR, Jaworowski A, et al. Differential expression of CD163 on monocyte subsets in healthy and HIV-1 infected individuals. PLoS One. 2011; 6:e19968. [PubMed: 21625498]
25. Estes JD, Harris LD, Klatt NR, Tabb B, Pittaluga S, Paiardini M, Barclay GR, et al. Damaged intestinal epithelial integrity linked to microbial translocation in pathogenic simian immunodeficiency virus infections. PLoS Pathog. 2010; 6:e1001052. [PubMed: 20808901]
26. Cummins AG, LaBrooy JT, Stanley DP, Rowland R, Shearman DJ. Quantitative histological study of enteropathy associated with HIV infection. Gut. 1990; 31:317–321. [PubMed: 2323596]
27. Heil F, Hemmi H, Hochrein H, Ampenberger F, Kirschning C, Akira S, Lipford G, et al. Species-specific recognition of single-stranded RNA via toll-like receptor 7–8. Science. 2004; 303:1526–1529. [PubMed: 14976262]
28. Schlee M, Roth A, Hornung V, Hagmann CA, Wimmenauer V, Barchet W, Coch C, et al. Recognition of 5′ triphosphate by RIG-I helicase requires short blunt double-stranded RNA as contained in panhandle of negative-strand virus. Immunity. 2009; 31:25–34. [PubMed: 19576794]
29. Iwasaki A, Pillai PS. Innate immunity to influenza virus infection. Nat Rev Immunol. 2014; 14:315–328. [PubMed: 24762827]
30. Wonderlich ER, Wijewardana V, Liu X, Barratt-Boyes SM. Virus-encoded TLR ligands reveal divergent functional responses of mononuclear phagocytes in pathogenic simian immunodeficiency virus infection. J Immunol. 2013; 190:2188–2198. [PubMed: 23338235]
31. Lissner D, Schumann M, Batra A, Kredel LI, Kuhl AA, Erben U, May C, et al. Monocyte and M1 macrophage-induced barrier defect contributes to chronic intestinal inflammation in IBD. Inflamm Bowel Dis. 2015; 21:1297–1305. [PubMed: 25901973]
32. Bain CC, Scott CL, Uronen-Hansson H, Gudjonsson S, Jansson O, Grip O, Guilliams M, et al. Resident and pro-inflammatory macrophages in the colon represent alternative context-dependent fates of the same Ly6Chi monocyte precursors. Mucosal Immunol. 2013; 6:498–510. [PubMed: 22990622]
33. Platt AM, Bain CC, Bordon Y, Sester DP, Mowat AM. An independent subset of TLR expressing CCR2-dependent macrophages promotes colonic inflammation. J Immunol. 2010; 184:6843–6854. [PubMed: 20483766]
34. Shen R, Richter HE, Clements RH, Novak L, Huff K, Bimczok D, Sankaran-Walters S, et al. Macrophages in vaginal but not intestinal mucosa are monocyte-like and permissive to human immunodeficiency virus type 1 infection. J Virol. 2009; 83:3258–3267. [PubMed: 19153236]
35. Shen R, Richter HE, Clements RH, Novak L, Huff K, Bimczok D, Sankaran-Walters S, et al. Macrophages in vaginal but not intestinal mucosa are monocyte-like and permissive to human immunodeficiency virus type 1 infection. Journal of virology. 2009; 83:3258–3267. [PubMed: 19153236]
36. Ploquin MJ, Silvestri G, Muller-Trutwin M. Immune activation in HIV infection: what can the natural hosts of simian immunodeficiency virus teach us? Curr Opin HIV AIDS. 2016; 11:201–208. [PubMed: 26845673]
37. Gueye A, Diop OM, Ploquin MJ, Kornfeld C, Faye A, Cumont MC, Hurtrel B, et al. Viral load in tissues during the early and chronic phase of non-pathogenic SIVagm infection. J Med Primatol. 2004; 33:83–97. [PubMed: 15061721]
38. Bigley V, McGovern N, Milne P, Dickinson R, Pagan S, Cookson S, Haniffa M, et al. Langerin-expressing dendritic cells in human tissues are related to CD1c+ dendritic cells and distinct from Langerhans cells and CD141high XCR1+ dendritic cells. J Leukoc Biol. 2015; 97:627–634. [PubMed: 25516751]

39. Fabriek BO, Dijkstra CD, van den Berg TK. The macrophage scavenger receptor CD163. Immunobiology. 2005; 210:153–160. [PubMed: 16164022]
40. Smith PD, Ochsenbauer-Jambor C, Smythies LE. Intestinal macrophages: unique effector cells of the innate immune system. Immunol Rev. 2005; 206:149–159. [PubMed: 16048547]
41. Hofer U, Schlaepfer E, Baenziger S, Nischang M, Regenass S, Schwendener R, Kempf W, et al. Inadequate clearance of translocated bacterial products in HIV-infected humanized mice. PLoS Pathog. 2010; 6:e1000867. [PubMed: 20442871]
42. Brenchley JM, Price DA, Schacker TW, Asher TE, Silvestri G, Rao S, Kazzaz Z, et al. Microbial translocation is a cause of systemic immune activation in chronic HIV infection. Nat Med. 2006; 12:1365–1371. [PubMed: 17115046]
43. McFaul SJ, Bowman PD, Villa VM, Gutierrez-Ibanez MJ, Johnson M, Smith D. Hemoglobin stimulates mononuclear leukocytes to release interleukin-8 and tumor necrosis factor alpha. Blood. 1994; 84:3175–3181. [PubMed: 7949190]
44. Schulbin H, Bode H, Stocker H, Schmidt W, Zippel T, Loddenkemper C, Engelmann E, et al. Cytokine expression in the colonic mucosa of human immunodeficiency virus-infected individuals before and during 9 months of antiretroviral therapy. Antimicrob Agents Chemother. 2008; 52:3377–3384. [PubMed: 18573939]
45. Cassol E, Rossouw T, Malfeld S, Mahasha P, Slavik T, Seebregts C, Bond R, et al. CD14(+) macrophages that accumulate in the colon of African AIDS patients express pro-inflammatory cytokines and are responsive to lipopolysaccharide. BMC Infect Dis. 2015; 15:430. [PubMed: 26475133]
46. Kwa S, Kannanganat S, Nigam P, Siddiqui M, Shetty RD, Armstrong W, Ansari A, et al. Plasmacytoid dendritic cells are recruited to the colorectum and contribute to immune activation during pathogenic SIV infection in rhesus macaques. Blood. 2011; 118:2763–2773. [PubMed: 21693759]
47. Fischer-Smith T, Tedaldi EM, Rappaport J. CD163/CD16 coexpression by circulating monocytes/macrophages in HIV: potential biomarkers for HIV infection and AIDS progression. AIDS Res Hum Retroviruses. 2008; 24:417–421. [PubMed: 18373432]
48. Thomas G, Tacke R, Hedrick CC, Hanna RN. Nonclassical patrolling monocyte function in the vasculature. Arterioscler Thromb Vasc Biol. 2015; 35:1306–1316. [PubMed: 25838429]
49. Kim WK, Sun Y, Do H, Autissier P, Halpern EF, Piatak M Jr, Lifson JD, et al. Monocyte heterogeneity underlying phenotypic changes in monocytes according to SIV disease stage. J Leukoc Biol. 2010; 87:557–567. [PubMed: 19843579]
50. de Baey A, Mende I, Baretton G, Greiner A, Hartl WH, Baeuerle PA, Diepolder HM. A subset of human dendritic cells in the T cell area of mucosa-associated lymphoid tissue with a high potential to produce TNF-alpha. J Immunol. 2003; 170:5089–5094. [PubMed: 12734354]
51. Dutertre CA, Amraoui S, DeRosa A, Jourdain JP, Vimeux L, Goguet M, Degrelle S, et al. Pivotal role of M-DC8(+) monocytes from viremic HIV-infected patients in TNFalpha overproduction in response to microbial products. Blood. 2012; 120:2259–2268. [PubMed: 22802339]
52. Byrareddy SN, Arthos J, Cicala C, Villinger F, Ortiz KT, Little D, Sidell N, et al. Sustained virologic control in SIV+ macaques after antiretroviral and alpha4beta7 antibody therapy. Science. 2016; 354:197–202. [PubMed: 27738167]
53. Patro SC, Pal S, Bi Y, Lynn K, Mounzer KC, Kostman JR, Davuluri RV, et al. Shift in monocyte apoptosis with increasing viral load and change in apoptosis-related ISG/Bcl2 family gene expression in chronically HIV-1-infected subjects. J Virol. 2015; 89:799–810. [PubMed: 25355877]
54. Wonderlich ER, Wijewardana V, Liu X, Barratt-Boyes SM. Virus-encoded TLR ligands reveal divergent functional responses of mononuclear phagocytes in pathogenic simian immunodeficiency virus infection. Journal of immunology. 2013; 190:2188–2198.
55. Doitsh G, Galloway NL, Geng X, Yang Z, Monroe KM, Zepeda O, Hunt PW, et al. Cell death by pyroptosis drives CD4 T-cell depletion in HIV-1 infection. Nature. 2014; 505:509–514. [PubMed: 24356306]
56. Murphey-Corb M, Wilson LA, Trichel AM, Roberts DE, Xu K, Ohkawa S, Woodson B, et al. Selective induction of protective MHC class I-restricted CTL in the intestinal lamina propria of

rhesus monkeys by transient SIV infection of the colonic mucosa. J Immunol. 1999; 162:540–549. [PubMed: 9886431]

57. Brown KN, Wijewardana V, Liu X, Barratt-Boyes SM. Rapid influx and death of plasmacytoid dendritic cells in lymph nodes mediate depletion in acute simian immunodeficiency virus infection. PLoS Pathog. 2009; 5:e1000413. [PubMed: 19424421]

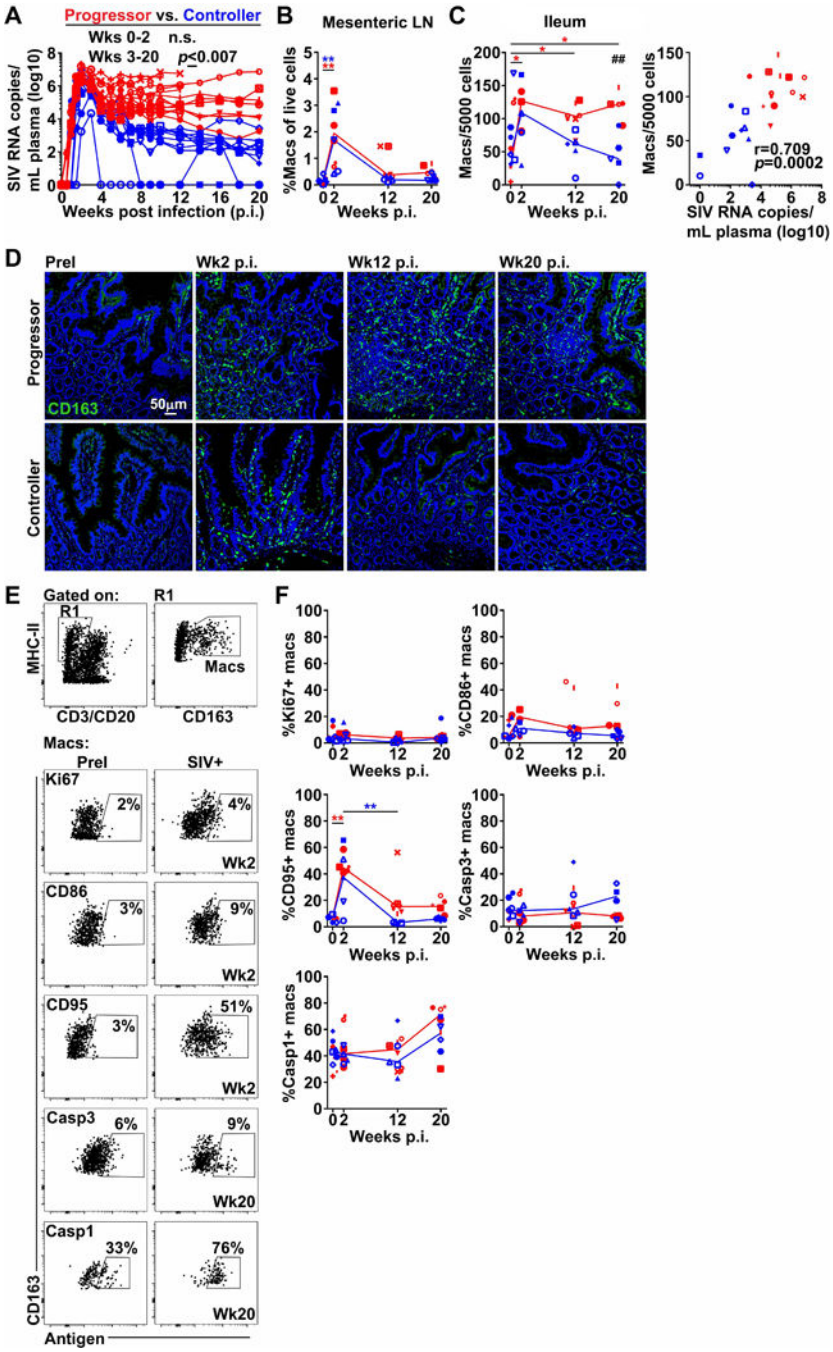

Figure 1. Persistent accumulation of CD163+ macrophages in ileum of SIV progressors but not controllers

(**A**) Longitudinal viral RNA burden in plasma. Red depicts macaques with week 8 viral loads >10^4 RNA copies/mL (SIV progressors) and blue depicts macaques with week 8 viral loads <10^4 RNA copies/mL (SIV controllers). (**B**) The proportion of CD163+ macrophages in mesenteric LNs as determined by flow cytometry. (**C**) (Left) The frequency of CD163+ macrophages in sections of ileum enumerated using ImageJ and MetaMorph software. (Right) Correlation between the frequency of gut macrophages and plasma viral loads at

weeks 12 and 20. (**D**) Representative immunofluorescence of sections of ileum from macaques prior to infection and at weeks 2, 12, and 20 post-infection stained with Ab to CD163 to identify macrophages. Original magnification = 200×. (**E**) (Top) Representative flow cytometric analysis of ileum single-cell suspensions showing gating strategy to define CD163+ macrophages. (Bottom) Representative flow cytometric analysis for Ki67, CD86, CD95, active caspase-3, and active caspase-1 on CD163+ macrophages in ileum before and after SIV infection. (**F**) The proportion of CD163+ macrophages expressing Ki67, CD86, CD95, active caspase-3, or active caspase-1 in ileum. Horizontal lines in (B), (C), and (F) represent medians. # signifies cross-sectional differences between progressors and controllers and * signifies longitudinal differences within the same groups. For (A) statistical comparisons were done using a two-tailed nonparametric Mann-Whitney U test. For (B), (C), and (F) statistical comparisons were done using a regular two-way ANOVA followed by Sidak's post test (#) or nonparametric one-way ANOVA followed by Dunn's post test (*). Correlations in (C) were determined using a two-tailed nonparametric Spearman rank test. */# $p < 0.05$; **/## $p < 0.01$; ***/### $p < 0.001$.

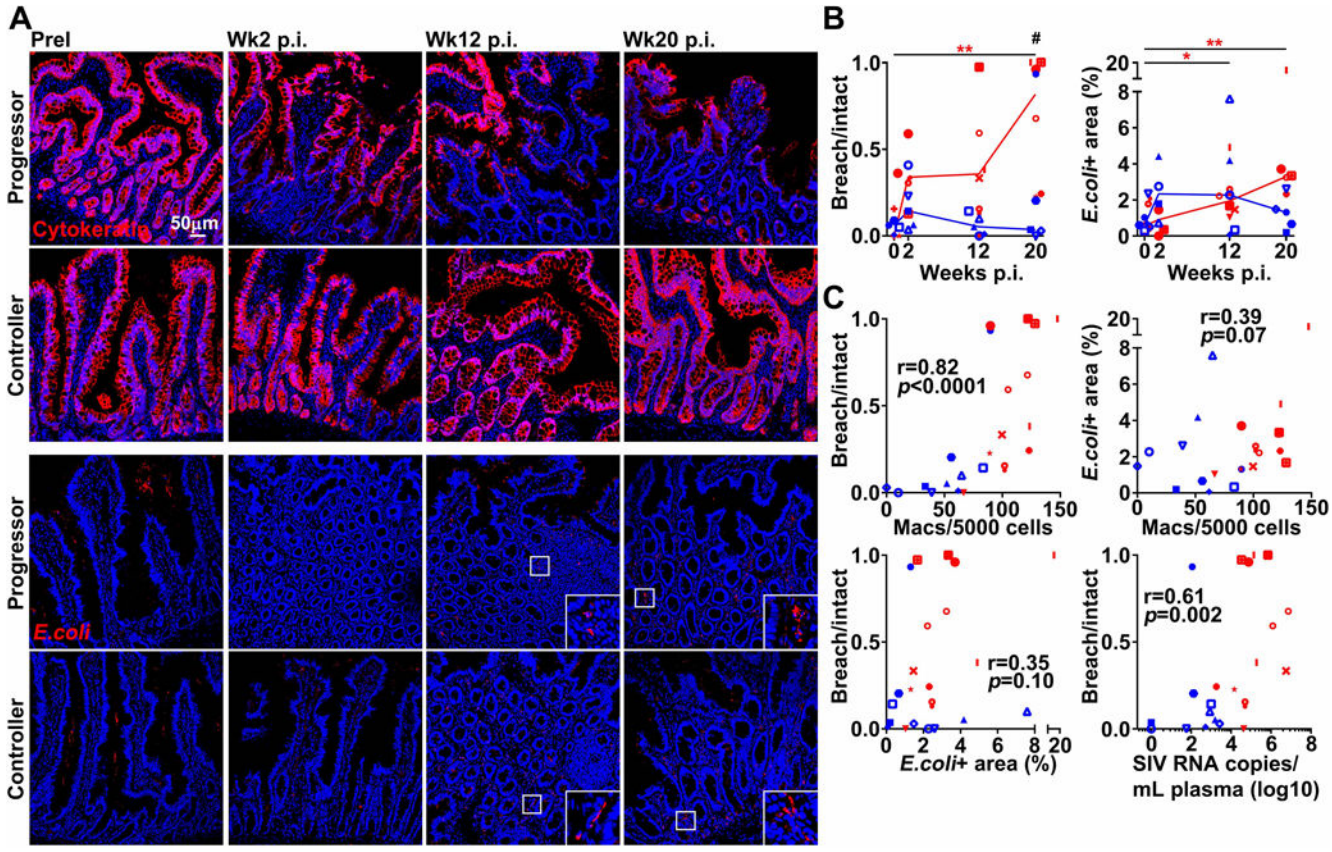

Figure 2. Progressive SIV infection is associated with gut epithelial damage and microbial translocation

(**A**) Representative immunofluorescence of ileum sections from macaques taken prior to infection and at weeks 2, 12, and 20 post-infection stained with Ab to cytokeratin (Top) or *E.coli* (Bottom) to identify epithelial integrity and extent of microbial translocation. Original magnification = 200×. (**B**) Quantitative image analysis showing ratio of breach to intact intestinal epithelium determined by cytokeratin+ staining (Left) and percentage of lamina propria occupied by *E.coli*+ staining (Right). Quantitation of cytokeratin+ staining and *E.coli*+ staining was carried out using NIS-Elements software. Horizontal lines in (B) represent medians. # signifies cross-sectional differences between progressors and controllers and * signifies longitudinal differences within the same groups. Statistical comparisons were done using a regular two-way ANOVA followed by Sidak's post test (#) or nonparametric one-way ANOVA followed by Dunn's post test (*). (**C**) Correlation between the ratio of breach to intact intestinal epithelium and the number of intestinal CD163+ macrophages, the percentage of lamina propria occupied by *E.coli* and the number of intestinal CD163+ macrophages, the ratio of breach to intact intestinal epithelium and the percentage of lamina propria occupied by *E.coli*, and ratio of breach to intact intestinal epithelium and plasma viral load at weeks 12 and 20. Correlations were determined using a two-tailed nonparametric Spearman rank test. Red depicts SIV progressors and blue depicts SIV controllers. */# $p < 0.05$; **/## $p < 0.01$; ***/### $p < 0.001$.

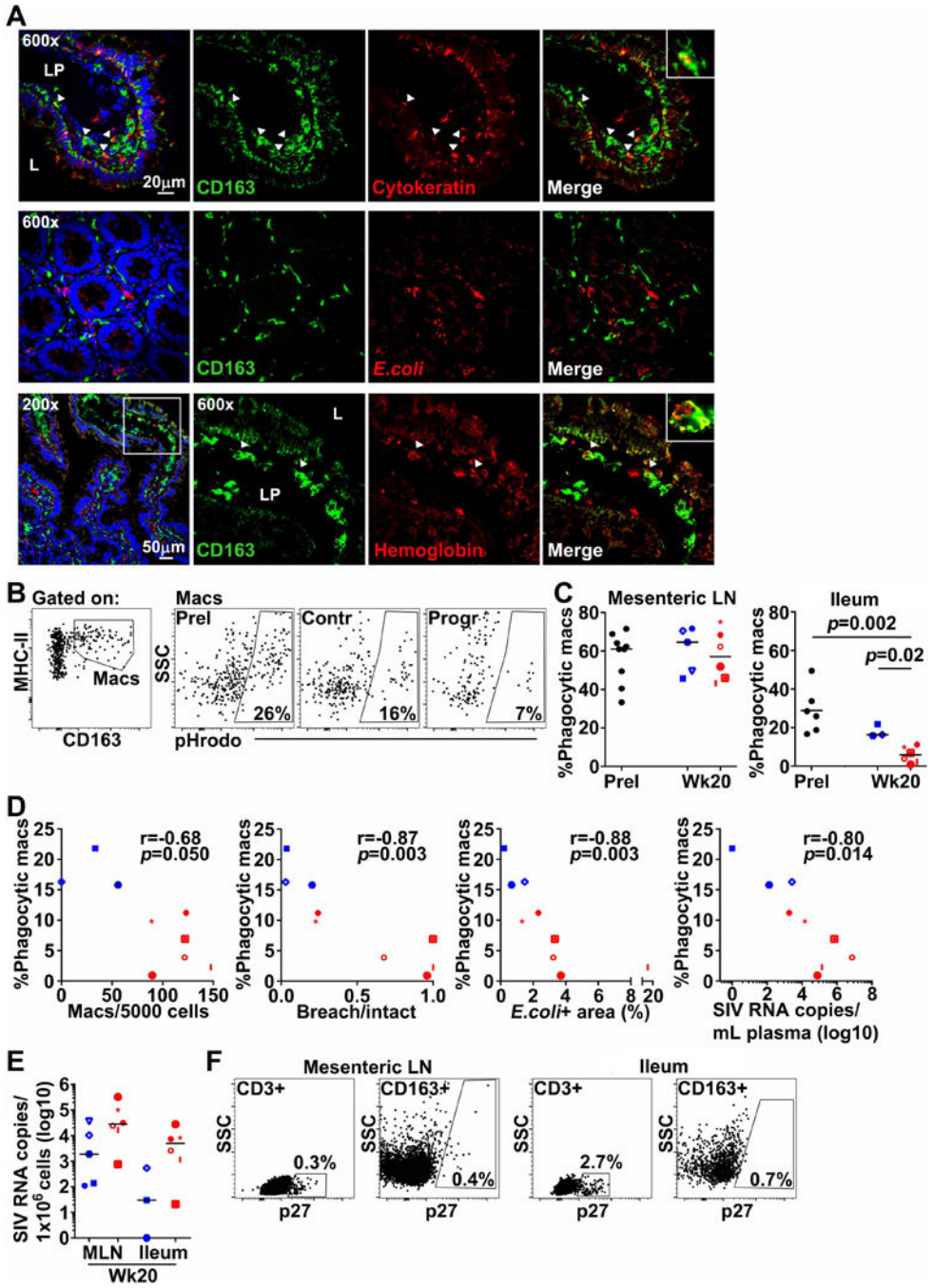

Figure 3. CD163+ gut macrophages from macaques with progressive SIV infection have impaired phagocytic function

(**A**) Representative immunofluorescence of ileum sections from SIV-infected macaques stained with Abs to CD163 and either cytokeratin to identify cytokeratin+ macrophages (Top), *E.coli* to identify *E.coli*+ macrophages (Middle), or hemoglobin to identify hemoglobin+ macrophages (Bottom). LP = lamina propria and L = lumen. (**B**) (Left) Representative flow cytometric analysis of ileum single-cell suspensions showing detection of CD163+ macrophages. (Right) Representative flow cytometric analysis for pHrodo on

CD163+ macrophages in ileum at pre-infection and at week 20 in high and low viral load samples. (**C**) Quantitation of pHrodo+ macrophages in mesenteric LNs (Left) and small intestine (Right) analyzed by flow cytometry at pre-infection and at week 20 in progressors and controllers. Statistical comparisons were done using two-tailed nonparametric Mann-Whitney U test. (**D**) Correlations between the percentage of pHrodo+ intestinal macrophages and the number of CD163+ macrophages per nucleated cells, the ratio of breach to intact intestinal epithelium, the density of *E.coli* in lamina propria, and plasma viral load at week 20. Correlations were determined using a two-tailed nonparametric Spearman rank test. (**E**) Quantitation of cell-associated viral RNA in mesenteric LNs and ileum at week 20. Horizontal bars in (C) and (E) represent medians. (**F**) Representative flow cytometric analysis of SIV-infected mesenteric LNs (Left) and ileum (Right) at week 20 showing staining for SIV p27 in CD3+ T cells and CD163+ macrophages. Red depicts SIV progressors and blue depicts SIV controllers. */# $p < 0.05$; **/## $p < 0.01$; ***/### $p < 0.001$.

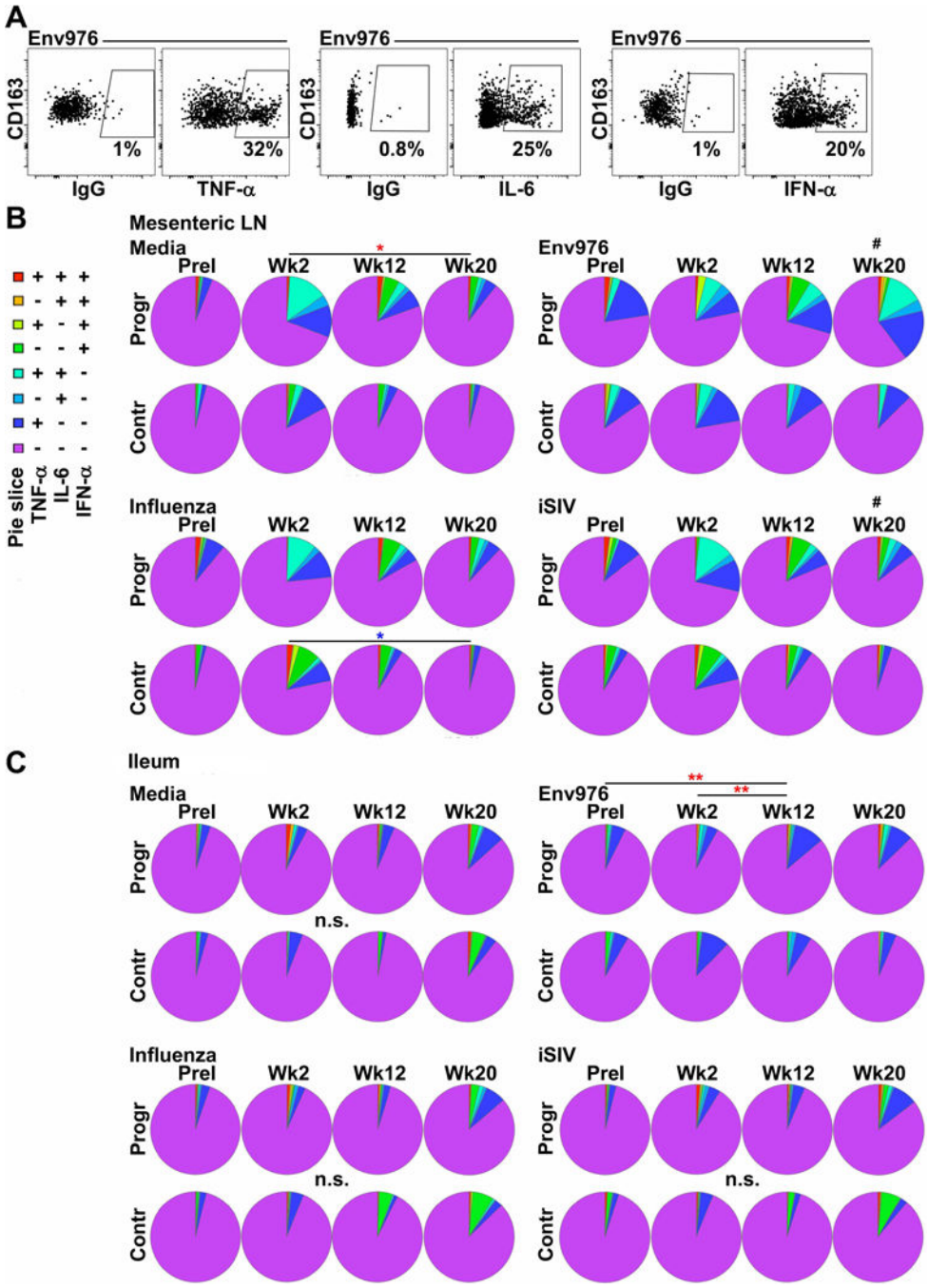

Figure 4. CD163+ gut macrophages are non-inflammatory and non-responsive to viral stimulation in SIV infection

(**A**) Representative flow cytometric analysis for CD163+ macrophages producing TNF-α, IL-6, and IFN-α in Env976 stimulated mesenteric LN single-cell suspensions. (**B, C**) SPICE analysis of the proportion of mesenteric LN (B) and intestinal (C) CD163+ macrophages producing different permutations of TNF-α, IL-6, and IFN-α prior to infection and at weeks 2, 12, and 20 post-infection either spontaneously or after stimulation by Env976, influenza, or iSIV. Statistical comparisons were done using a permutation test performed with SPICE

software. # signifies cross-sectional differences between progressors and controllers and * signifies longitudinal differences within the same groups. Red asterisks reflect SIV progressors and blue asterisks reflect SIV controllers. */# $p < 0.05$; **/## $p < 0.01$; ***/### $p < 0.001$.

Table 1

Animal characteristics

Animal ID	MHC class I haplotype			Wk8 plasma VL (RNA copies/mL)
Predicted SIV Controllers (VL <10^4 RNA copies/mL)				
M12-13	B*008+	A*001+	B*017+	<200
M174-12	B*008+	A*001+	B*017−	2,702
M11-13	B*008+	A*001+	B*017−	1,953
M13-13	B*008+	A*001+	B*017−	1,542
M57-13	B*008+	A*001−	B*017−	435
M58-13	B*008+	A*001−	B*017−	1,632
M175-12	B*008+	A*001−	B*017−	<200
M176-12	B*008+	A*001−	B*017−	2,669
M177-12	B*008+	A*001−	B*017−	1,422
M132-14	B*008−	A*001−	B*017−	1,305
Median				**1,482**
Predicted SIV Progressors (VL >10^4 RNA copies/mL)				
M59-13	B*008+	A*001−	B*017−	21,802
M60-13	B*008+	A*001−	B*017−	22,826
M173-12	B*008+	A*001−	B*017−	168,148
M131-14	B*008−	A*001−	B*017−	636,401
M133-14	B*008−	A*001−	B*017−	79,026
M134-14	B*008−	A*001−	B*017−	48,212
M135-14	B*008−	A*001−	B*017−	15,110
M136-14	B*008−	A*001−	B*017−	289,716
M172-12	B*008−	A*001−	B*017−	4,000,000
M181-13	B*008−	A*001−	B*017−	2,400,000
M182-13	B*008−	A*001−	B*017−	410,006
M183-13	B*008−	A*001−	B*017−	44,017
M184-13	B*008−	A*001−	B*017−	38,742
M185-13	B*008−	A*001−	B*017−	50,000
Median				**64,513**